Striped and Spotted Pattern Generation on Reaction-diffusion Cellular Automata

Tetsuya Asai
Graduate School of Information Science and Technology, Hokkaido University,
Kita 14, Nishi 9, Kita-Ku, Sapporo 060-0814, Japan.

Abstract— **A novel reaction-diffusion cellular-automaton model that generates Turing-like spatial patterns is proposed. The model employs linear diffusion fields of activators and inhibitors and a discrete transition rule after diffusion. Theoretical analysis of the one dimensional model proved that i) spatial distribution given by a periodic square function is stable at the equilibrium and ii) the spatial frequency is inversely proportional to the square root of a diffusion coefficient of the inhibitors.**

I. Introduction

In the process of ontogeny in a multicellular organism, the organism develops from a fertilized egg into matured differentiated cell groups, through repeated division/differentiates. Turing [1] suggested the concept of "Diffusion (driven) instability" for phenomena in systems where diffusion is able to enhance transition from a homogeneous state to a spatially in-homogeneous stable state. In his framework, time development in the system is described by the sum of reaction and diffusion. The former represents local production/extinction of the substance or state and the latter represents a transport process, which tends to dampen any inhomogeneity of the neighboring region, called the reaction-diffusion (RD) system. He gave an example where the spatial instability of a spatial homogeneous structure could take place through the addition of the diffusion effect. This Turing RD model is well known as one in which stable striped or spotted patterns are generated.

There are many ordered complex patterns in nature. For example, one can see patterns in animal skins where the patterns are formed spontaneously. Turing's and modified RD models have been studied because of their significance in explaining pattern formations on animal skins. Striped patterns can not only be seen in animal skin but also human fingerprints. Fingerprint patterns give us important cues for distinguishing individuals. Recent progress with digital microprocessors will certainly push advances in intelligent security systems that recognize fingerprints patterns. This paper deals with the basic mechanism and implementation of restoring striped/spotted patterns.

II. Model and the Theoretical Analysis

The RD system is a complex system in which the reaction and diffusion of chemical species coexist under nonequilibrium conditions. It produces a variety of orders, rhythms, and self-organizing phenomena observed in nature and in life. Typical examples of such patterns are marking patterns on various animals, which are referred to as Turing patterns [2], [3].

Turing patterns can usually be obtained by solving mathematical RD models described by a set of partial differential equations (PDE) that are represented by continuous spatiotemporal variables. Several attempts to reproduce Turing patterns with limited computational resources have been made over the years [4], [5], [6], [7], [8], [9]. A typical example is the use of cellular automata (CA) where the space is separated by a set of discrete cells, and time and cell state are represented by discrete values. Gerhardt, Schuster and Tyson have discretized the RD model based on chemical system [5], [6]; Markus and colleagues have shown the way to avoid unisotropy of the pattern and described various shell patterns [7]; Weimar, Tyson, and Watson have generalized CA model based on RD model and evaluated CA in relation to PDE [8], [9]. In the way to construct CA model, simplifying the nonlinear dynamics in a continuous RD model is a difficult task because the differential equations are rewritten by conditional divergence rules in the CA.

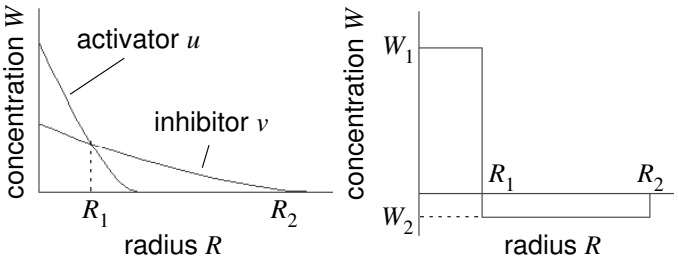

Fig. 1. Diffusion of activators and inhibitors on (a) continuous model and (b) discrete model.

Young [4] proposed a simplified discrete CA model for describing Turing patterns. He introduced a discrete model for diffusion effects between chemical substances and represented all the states (usually they had two variables; i.e., activators and inhibitors) with a single binary {1,0} variable. Then, he further simplified the diffusion of the two chemical substances.

One necessary condition for generating Turing patterns is that activators only influence their local neighbors (hard to diffuse), while inhibitors not only influence their neighbors but distant cells (easy to diffuse). Figure 1(a) illustrates the diffusion profile of activators and inhibitors in a continuous model, where R represent the distance from the center of diffusion, R_1 the position where activators and inhibitors have the same concentration, and R_2 the position where the concentration of inhibitors is asymptotically zero. When $R < R_1$, activators and inhibitors produce "active effects" on the field because the concentration of activators is higher than that of inhibitors. When $R_1 < R < R_2$, they produce "inhibitory effects" because the concentration of inhibitors is higher.

Young simplified the effects on distance R as illustrated in Fig. 1(b). In his CA model, a cell whose state is "1" within $R < R_1$ has positive effects W_1, while a cell whose state is "1" within $R_1 < R < R_2$ has negative effects W_2. The transition of a cell in position $\mathbf{r}$ is determined by the weighted-sum of cells within $R < R_2$ whose states are "1" expressed as $\sum_{|\mathbf{r}-\mathbf{r_i}|\leq R_2} W$, where W represents the weight strength. If the summed value is zero, no transition occurs, while if the value is positive (or negative), the subsequent state of the cell is set to "1" (or "0"). This *step* transition rule corresponds to chemical reactions in continuous

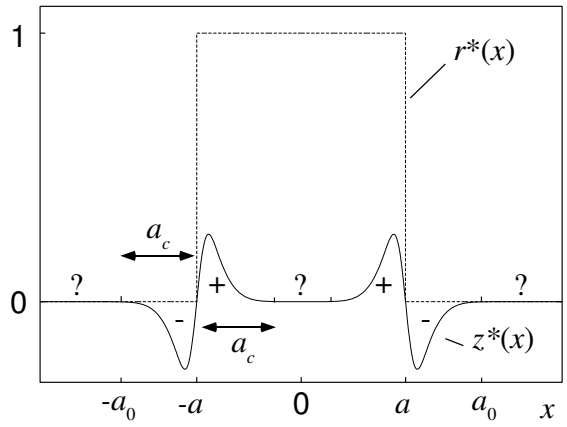

Fig. 2. DoG responses of proposed model for single square-pulse input.

RD models. Young showed that stripe patterns and then spot patterns appeared on the CA with fixed R_1, R_2 and W_1 by changing the value of W_2. Surprisingly, all the patterns became stable within 10 steps, even when random initial patterns were given to the CA.

A. A modified RD CA model

In Young's simplified CA, the diffusion terms in the continuous RD model are represented by the weighted summation of neighboring cells, while the reaction terms in the RD model are represented by the sign of the sum. Therefore, to describe a cell's transition, the cell has to refer to its neighboring cell's states. Since the number of neighboring cells is approximately calculated by $\pi \times R_2 \times R_2$, the number of physical connection wires (on CA hardware) to refer the neighboring cell's states increases significantly when R_2 increases. Moreover, the CA cannot generate spatially smooth patterns because step functions are used in the cell transition rule. A promising solution to these problems is using a discrete diffusion equation with a four-point spatial approximation method and an analog sigmoid function in the rule instead of the step function.

The weighted-summing computation described above is done by the diffusion fields. In other words, activators and inhibitors diffuse in individual diffusion fields and are then convoluted by a 2D array of cells. Each cell's state is determined by the difference between the concentration of activators, u, and inhibitors, v, at a given spatial point, (x, y). Diffusion equations for variables u and v are integrated for time δt. Then a cell's subsequent state is determined by the value of the sigmoid function for $u - v$. The dynamics can be formulated as

1. (Diffusion)
   $\partial u(\mathbf{r}, t)/\partial t = D_u \nabla^2 u(\mathbf{r}, t)$,
   $\partial v(\mathbf{r}, t)/\partial t = D_v \nabla^2 v(\mathbf{r}, t)$,
2. (Reaction)
   $u(\mathbf{r}, \delta t(n+1)) = v(\mathbf{r}, \delta t(n+1)) = f\big(u(\mathbf{r}, \delta t \cdot n) - v(\mathbf{r}, \delta t \cdot n) - c\big)$,
   $f(x) = \big(1 + \exp(-\beta x)\big)^{-1}$,

where n represents the time step, $\mathbf{r} = (x, y)$, c is the offset value of the sigmoid function, and β is the slope of the function. Let us define this sequential operation as "one cycle". In the following, we see that the system produces spatiotemporal patterns by repeating this cycle.

B. Theoretical Analysis

Here let us analyze operations for the proposed model in 1D space and reveal the relation between the spatial frequency of equilibrium patterns and diffusion coefficients.

Since an impulse response of a diffusion equation is represented by the Gaussian, that of $u - v$ is given by a 'difference of Gaussian' (DoG) function:

$$\mathrm{DoG}(x,t) = \frac{1}{\sqrt{4\pi t}}\left[\frac{1}{\sqrt{D_u}}\exp\left(\frac{-x^2}{4D_u t}\right) - \frac{1}{\sqrt{D_v}}\exp\left(\frac{-x^2}{4D_v t}\right)\right], \tag{1}$$

where x represents the space. Differential distribution $u - v$, after activators and inhibitors are diffused for time δt, is thus given by

$$z_n(x) \equiv \int_{-\infty}^{\infty} r_n(x - X) \cdot \mathrm{DoG}(X, \delta t)\, dX, \tag{2}$$

where $r_n(x)$ represents an initial input to u and v at the n-th cycle. Therefore, the dynamics of the proposed model can be represented by

$$r_{n+1}(x) = f[z_n(x)], \tag{3}$$

where $r_{n+1}(x)$ represents the subsequent initial input. Assuming the equilibrium state, we obtain

$$r^*(x) = f[z^*(x)], \quad z^*(x) = \int_{-\infty}^{\infty} r^*(x-X)\cdot\mathrm{DoG}(X, \delta t)\, dX, \tag{4}$$

where $z^*(x)$ and $r^*(x)$ represent the equilibrium distribution of $u-v$ and the resulting sigmoid outputs. Assume the equilibrium distribution is

$$r^*(x) = \begin{cases} 1 & (-a < x < a) \\ 0 & (\text{else}), \end{cases} \tag{5}$$

where $a > 0$. For this input, we obtain

$$z^*(x) = \int_{x-a}^{x+a} \mathrm{DoG}(X, \delta t)\, dX = \frac{1}{2}\left[\mathrm{erf}\left(\frac{x+a}{p_u}\right) - \mathrm{erf}\left(\frac{x-a}{p_u}\right) - \mathrm{erf}\left(\frac{x+a}{p_v}\right) + \mathrm{erf}\left(\frac{x-a}{p_v}\right)\right], \tag{6}$$

where $p_{u,v} \equiv \sqrt{4D_{u,v}\delta t}$ and $\mathrm{erf}(\cdot)$ represents the error function. To ensure that input $r^*(x)$ is stable, $z^*(x)$ must be positive for $-a < x < a$, and be negative for other x. Figure 2 plots function $z^*(x)$ for given $r^*(x)$ when $D_u = 0.01$, $D_v = 0.1$, $\delta t = 0.01$, and $a = 0.2$. In this example, we see that the sign of $z^*(x)$ for the center ($x \approx 0$) and surrounds ($|x| > a_0$ in the figure) is indefinite because of $z^*(x) \approx 0$ in these regions. This results in unstable $r^*(x)$ at $x \approx 0$ and $|x| > a_0$.

An error function can be represented in the form of a normal (Gaussian) distribution

$$\frac{\mathrm{erf}(x)}{2} = \int_0^{\sqrt{2}\sigma x} \frac{1}{\sqrt{2\pi}\sigma}\exp\Big(-\frac{y^2}{2\sigma^2}\Big)dy, \tag{7}$$

where σ^2 represents the variance. Using the 3σ law of the Gaussian, we can approximately obtain the values of x where $z^*(x) \approx 0$ as

$$x = -a - \frac{3p_v}{\sqrt{2}},\ -a + \frac{3p_v}{\sqrt{2}},\ a - \frac{3p_v}{\sqrt{2}},\ \text{and}\ a + \frac{3p_v}{\sqrt{2}}, \tag{8}$$

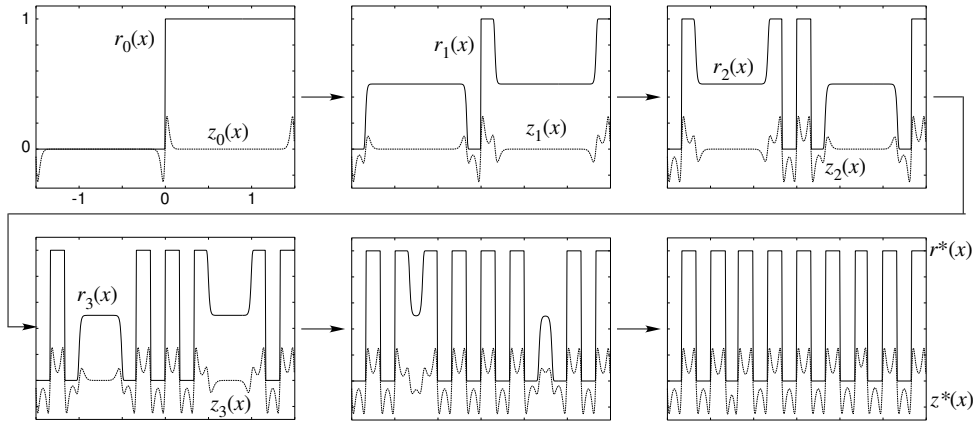

Fig. 3. Pattern formation on 1D model.

which indicates that the region $-2a \le x \le 2a$ of $r^*(x)$ is stable as long as $a \le 3p_v/\sqrt{2}$ ($\equiv a_c$). Therefore, for a periodic square-wave input,

$$r^*(x) = \begin{cases} 1 & \Big((4n-1)a < x < (4n+1)a\Big), \quad (n = 0, \pm 1, \pm 2, \ldots) \\ 0 & (\text{else}), \end{cases} \tag{9}$$

whose primary spatial frequency f_0 is given by $1/4a$, I conclude that a square wave of $f_0 \ge 1/4a_c = \sqrt{2}/12p_v$ is stable in the subsequent cycle.

For periodic waves of $f_0 < 1/4a_c$, regions of x where $z^*(x) \approx 0$ will exist, which results in $r^*(x) \approx 0.5$ (not 0 or 1). Let us estimate this region by employing piecewise linear function $f_{\rm pwl}(\cdot)$ instead of sigmoid function $f(\cdot)$. Because $df/dx|_{x=0} = \beta/4$, we obtain

$$f(x) \approx f_{\rm pwl}(x) \equiv \begin{cases} \beta x/4 + 0.5 & (-2/\beta \le x \le 2/\beta) \\ 1 & (x > 2/\beta) \\ 0 & (x < -2/\beta), \end{cases} \tag{10}$$

which means that $r^*(x)$ will not take 0 or 1 when $-2/\beta \le z^*(x) \le 2/\beta$. Therefore, the value of x where $z^*(x) = \pm 2/\beta$ determines stable wave frequency. To calculate this, the following $z^*(x)$ is considered,

$$z^*(x) = \frac{1}{2}\left[\mathrm{erf}\left(\frac{x+a}{p_u}\right) - \mathrm{erf}\left(\frac{x+a}{p_v}\right)\right], \tag{11}$$

around $x = -a$ for simplicity. When the argument of the error function is large, the following asymptotic expansion can be used:

$$\mathrm{erf}(x) \approx 1 - \frac{1}{x\sqrt{\pi}}\exp(-x^2). \tag{12}$$

Therefore, when $p_u \ll p_v$ ($d_u \ll d_v$), one has

$$z^*(x) \approx \frac{1}{2\sqrt{\pi}}\left[\frac{p_v}{x+a}\exp\left(-\frac{(x+a)^2}{p_v^2}\right)\right]. \tag{13}$$

The value of x where $z^*(x_0) = 2/\beta$ is thus given by

$$x_0 = p_v\sqrt{\frac{F(2/k^2)}{2}} - a, \tag{14}$$

where $k \equiv 4\sqrt{\pi}/\beta$ and $F(\cdot)$ represents the inverse function of Lambert's W function. Therefore, I conclude that i) $r^*(x)$ is not stable when the wavelength is larger than $2x_0$ and ii) the stable wavelength is proportional to p_v (square root of D_v).

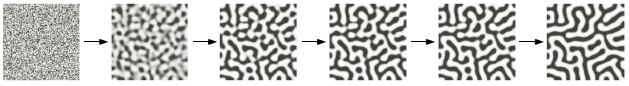

Fig. 4. Snapshots of stripe-pattern formation observed with proposed model.

Figure 3 has the simulation results for $\delta t = 0.01, D_u = 0.01, D_v = 0.1$ and $\beta = 10^4$ with a cyclic boundary condition. Step input was given at the initial cycle. After a few iterations, a stable square wave appeared. The primary spatial-frequency agreed well with the theoretical prediction ($f_0 = 0.5x_0$). Furthermore, by changing the values of D_v, I numerically confirmed that the equilibrium wave frequency is inversely proportional to the square root of D_v.

Figure 4 is an example of striped pattern formation on a 2D model ($D_v/D_u = \beta = 10$, $c = 0$, $\delta t = 1$). The values of $f\big(u(\mathbf{r}, \delta t{\cdot}n) - v(\mathbf{r}, \delta t{\cdot}n) - c\big)$ are represented on a grayscale ($f(\cdot) = 0$: black, $f(\cdot) = 1$: white). The initial state was randomly set within the values of [0:1]. After approximately 10-cycle updates, a stable striped pattern was generated. The space was filled with striped patterns according to the initial spatial distribution. Therefore, if a striped pattern such as a fingerprint pattern is given to the CA, local patterns that do not fit the striped global patterns are replaced with striped patterns based on the global patterns.

Figure 5 shows a pattern diagram for two variable parameters (D_v/D_u and c). When the value of c was increased, the resulting patterns changed from black spotted to white spotted via the stripe patterns. Also, the spatial frequency could be controlled by the value of D_v/D_u. That is, one can control the form of target patterns (spotted or striped) and the spatial resolution with these two parameters.

Physically, parameter c represents a total balance of activators u and inhibitors v in the model. When $c > 0$, v is predominant over u because the values of u must be larger than that of $v + c$ to ensure $f(u - v - c) > 0.5$, and vice versa when $c < 0$. This can easily be confirmed from Fig. 5 where the area occupied by inhibitors (black areas) is equal to the area occupied by activators (white) when $c = 0$, while inhibitors (black areas) become predominant as c increases.

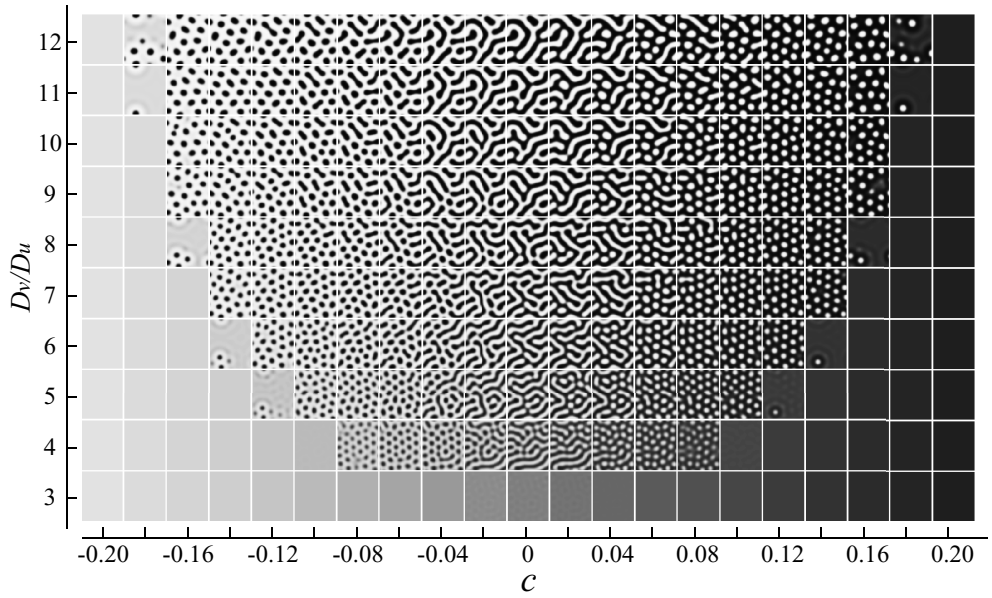

Fig. 5. Pattern diagram for proposed RD model.

III. Summary and Discussion

A novel reaction-diffusion (RD) cellular-automaton model that generates Turing-like spatial patterns was proposed based on continuous diffusion fields and an analog state variable to Young's local activator-inhibitor model [4]. The model employed linear diffusion fields of activators and inhibitors and a discrete transition rule after diffusion. Theoretical analysis of the one dimensional model proved that i) spatial distribution given by a periodic square function is stable at the equilibrium and ii) the spatial frequency is inversely proportional to the square root of a diffusion coefficient of the inhibitors.

What is a RD processor? A traditional RD processor is a real 'liquid' medium, usually composed of a thin layer of solution or gel containing chemical reagents, that in its space-time dynamics transforms data to results in a sensible and programmable way. Data, to be processed, can be represented by the concentration of certain reagents and spatial structures, e.g., diffusive or excitation waves, spread from these initial data points. The spreading patterns interact to produce either stationary structures, e.g., a precipitate concentration profile, or dissipative structures, e.g., oscillating patterns. The final state, or even just a particular spatial state of the whole medium, represents a result of the RD computation.

Recently, a great deal of attention has been paid to the study of the computational properties of spatially extended chemical systems. To date, it has been proved experimentally that RD chemical processors are capable of computing shortest paths, image processing, computational geometry, pattern recognition and logical computation. In the last ten years enough results have been obtained to demonstrate that RD chemical processors are not simply curiosities invented by theoreticians but promising — and somewhat revolutionary — computing architectures offering an alternative to the as yet unchallenged domination of the current silicon designs. This is because spatially extended RD processors are equivalent to massively parallel computers.

A two-dimensional RD processor, implemented in a thin-layer liquid phase in a Petri dish, consists of millions of micro-volumes, nearly 10^{19}. The concentrations of reactants in each micro-volume are changed in parallel depending on reagent concentrations in neighbouring micro-volumes. Therefore, a thin layer of a chemical medium could be seen as an (ir)regular array of elementary few-bit processors. The great number of elementary processing units makes chemical computers tolerant to impurities of RD media while local connectivity allows for localisation of spatial inhomogeneities in the reacting medium. The 'amorphous' structure of the chemical medium guarantees that a massively parallel chemical processor will self-reconfigure and restore its original architecture after some parts of the physical processing medium are removed.

Acknowledgments

The author wish to thank Dr. Ikuko N. Motoike of Future University - Hakodate for her invaluable discussions and suggestions during my research. This study was partly supported by Industrial Technology Research Grant Program in '02 and '04 from New Energy and Industrial Technology Development Organization (NEDO) of Japan.

References

[1] Turing, A.M. The chemical basis of morphogenesis. Phil. Trans. R. Soc. Lond. **B 237** (1952) 37–72.

[2] Nicolis, G. & Prigogine, I.: Self-organization in Nonequilibrium Systems — From Dissipative Structures to Order through Fluctuations. John Wiley & Sons, Inc., New York (1977).

[3] Murray, J.D.: Mathematical Biology I & II (3rd Ed.). Springer, New York (2002).

[4] Young, D.A. A local activator-inhibitor model of vertebrate skin patterns. Math. Biosci. **72** (1984) 51–58.

[5] Gerhardt M. & Schuster H., A cellular automaton describing the formation of spatially ordered structures in chemical systems. Physica D. **36** (1989) 209–221.

[6] Gerhardt M., Schuster H. & Tyson J. J., A cellular automaton model of excitable media II. Curvature, dispersion, rotating waves and meandering waves. Physica D **46** (1990) 392–415.,

[7] Markus M. & Hess B., Isotropic cellular automaton for modeling excitable media. Nature, **347** (1990) 56–58,

[8] Weimar J. R., Tyson J. J., & Watson L. T., Diffusion and Wave Propagation in Cellular Automata Models for Excitable Media. Physica D **55** (1992) 309–327,

[9] Weimar J. R. & Boon J.-P., Class of Cellular Automata for Reaction-Diffusion Systems. Phys. Rev. E **49** (1994) 1749–1752.

[10] Schepers H. & Markus M., Two types of performance of aniIsotropic cellular automaton: stationary (Turing) patterns and spiral waves. Physica A **188** (1992) 337–343,

[11] Kusch I. & Markus M., Mollusc shell pigmentation: cellular automaton simulations and evidence for undecidability. J. Theor. Biol. 178, 333-340 (1996).